Science and Technology Indonesia
e-ISSN:2580-4391 *p*-ISSN:2580-4405
Vol. 10, No. 4, October 2025

Research Paper

Cu Film Characteristics Synthesized Using Electrodeposition Technique at Various Currents and Under a Rotating Neodymium Magnet

Ferry Budhi Susetyo[1*], Basori[2], Muhd Ridzuan Mansor[3,4], Ruliyanta[5], Sigit Dwi Yudanto[6], Cahaya Rosyidan[7], Evi Ulina Margareta Situmorang[8], Daniel Edbert[9], Etty Mutiara[10], Tri Yulianto[10], Agus Jamaludin[10], Dwi Nanto[11]

[1]*Department of Mechanical Engineering, Universitas Negeri Jakarta, Jakarta, 13220, Indonesia*
[2]*Department of Mechanical Engineering, Universitas Nasional, Jakarta, 12520, Indonesia*
[3]*Faculty of Technology Mechanical and Engineering, Universiti Teknikal Malaysia Melaka, Melaka, 76100, Malaysia*
[4]*Centre for Advanced Research on Energy, Universiti Teknikal Malaysia Melaka, Melaka, 76100, Malaysia*
[5]*Department of Electrical Engineering, Universitas Nasional, Jakarta, 12520, Indonesia*
[6]*Research Center for Metallurgy, National Research and Innovation Agency, Tangerang Selatan, 15314, Indonesia*
[7]*Department of Petroleum Engineering, Universitas Trisakti, Jakarta, 11440, Indonesia*
[8]*Department of Physiology School of Medicine and Health Sciences, Atma Jaya Catholic University of Indonesia, Jakarta, 14440, Indonesia*
[9]*Department of Microbiology School of Medicine and Health Sciences, Atma Jaya Catholic University of Indonesia, Jakarta, 14440, Indonesia*
[10]*Research Center for Nuclear Material and Radioactive Waste Technology, National Research and Innovation Agency, Tangerang Selatan, 15314, Indonesia*
[11]*Department of Physics Education, UIN Syarif Hidayatullah, Jakarta, 15412, Indonesia*
*__Corresponding author__: fbudhi@unj.ac.id

Abstract
In the present study, Cu films were made over Al alloy using the electrodeposition technique. Electrodeposition conducted at various currents (80, 100, and 120 mA), with and without influence by a rotating magnetic field (100 rpm of rotation). 0.5 M $CuSO_4$ + 20 mL of H_2SO_4 was used for electrolyte solutions. The sample before and after electrodeposition was weighed using digital scale to calculate deposition rate and current efficiency. All formed Cu films were characterized using X-ray diffraction (XRD), attenuated total reflectance Fourier transform infrared spectroscopy (ATR-FTIR), Scanning electron microscopy equipped with Energy dispersive spectroscopy (SEM-EDS), and Potentiostat apparatus. Furthermore, antibacterial activity using *Staphylococcus aureus* was also investigated. Increasing the current of electrodeposition leads to an increase in deposition rate and current efficiency for both conditions (with and without rotating magnetic field influence). Based on the XRD and ATR-FTIR investigation, Cu was successfully deposited onto Al surface. Currents used for the electrodeposition process between 80-100 mA would result in a faceted structure, while using 120 mA results near to spheroidal. Shifting to higher currents leads to decreases in grain sizes and presenting a rotating magnetic field also enhances the grain size. Current and rotating magnetic influences are not linearly influencing corrosion potential, corrosion rate and antibacterial activity. The sample made using higher current plus influencing with a rotating magnetic field has less corrosion rate and higher area of inhibition at around 0.808 mmpy and 4.01 cm^2.

Keywords
Cu Films, Electrodeposition, Magnetic Field, Corrosion, Inhibition, Antibacterial Activity

Received: 14 April 2025, Accepted: 28 July 2025
https://doi.org/10.26554/sti.2025.10.4.1156-1168

1. INTRODUCTION

Aluminum (Al) alloy, covered using Copper (Cu) film, could transform it into an antimicrobial material. Cu could act as an antibacterial material due to Cu ions releasing would kill bacteria (Arendsen et al., 2019). Despite Cu could kill the bacteria, the Cu in the form of film has more killing the bacteria than the sheet (Sharifahmadian et al., 2013). Therefore, coating Al with Cu seems like a promising way to create antibacterial materials through the electrodeposition process (Augustin et al., 2016a). Besides Cu, Zinc (Zn) also could be used as an antibacterial material property which could inhibit growth and killing bacteria. Unfortunately, according to Raja et al. (2023) *Staphylococcus aureus* is still seen after 24 hours contact observations using Zn as an antibacterial. Moreover, Cu has more killing than Zn for 2, 6, and 24 hours of incubation time.

To create Cu film through the electrodeposition process two parameters, it needs to be considered as current where applied and magnetic has influences (Augustin et al., 2016a;

Syamsuir et al., 2023b). An increase in the current leads to an increase in a throwing power, deposition rate and current efficiency (SEAKR, 2017; SEKAR, 2017). Presenting a magnetic field also could increase the deposition rate and current efficiency due to the exhibit of a magnetohydrodynamic (MHD) flow convection (Chiba et al., 1988; Wang et al., 2015). Interestingly, magnetic position (parallel or vertical) where placed during electrodeposition could change interface transfer resistance of the film (Liu et al., 2022). Different pole of the magnet used during electrodeposition process could also influence formed microstructure (Murdoch et al., 2018). Moreover, an increase in deposition rate and current efficiency could be resulting diverse surface morphology, grain size and surface roughness (Armini, 2011; Ibañez and Fatás, 2005; Niu et al., 2015; Wang et al., 2015). Hence, it could influence the area of inhibition size because larger surface area would release more Cu ions into the environment and increase the inhibition area (Motshekga, 2024; Shim et al., 2015; Tavakoli et al., 2019).

Several researchers focused on varied current. Armini (2011) conducted an electrodeposition of Cu using 0.04 M $CuSO_4$ and found that an increase in the current density (from 3 to 4 mA/cm^2) leads to an increase in the surface roughness of Cu film. Augustin et al. (2016a) and Augustin et al. (2016b) carried out Cu electrodeposition on an Al substrate with variations in current density of 200, 400, 600, 800, and 1000 A/m^2 resulting in: (111) plane, Full width at half maximum (FWHM) between 0.2380-0.3152, crystal size around 66-35.5 nm, and 70 to 93° of water contact angle. SEAKR (2017) has conducted Cu electrodeposition using electrolyte solution containing 100 g/L $Cu(CH_3COO)_2$, 90 mL/L CH_4O_3S, 20 g/L $C_2H_3NaO_2$ and 0.25 g/L $C_{12}H_{18}Cl_2N_4OS$ at various current density (1, 2, 3, 4, and 5 A/cm^2) and found increase in current density led to increase in throwing power and current efficiency. Goranova et al. (2016) performing electrodeposition Ni−Cu using 4 and 10 A/dm^2 of current densities resulting different surface morphology.

Electrodepositions where influencing using a rotating magnet is still limited, especially for the Cu electrodeposition. Wang and Chen (2015) conducting electrodeposition of nickel (Ni) influenced by the rotating magnetic field (1000-3000 rpm) and resulting decrease rotation that could increase the surface roughness of the forming films. Ji et al. (2020) found a more uniform SiC distribution by presenting a rotating magnetic field in the electrodeposition of Ni−SiC. A previous study found that a rotating magnetic field could make the Ni films more uniform when conducting electrodeposition of Ni (Syamsuir et al., 2023b). Another previous study has found that decreasing in the magnetic rotation speed could change the surface morphology of the Cu film from faceted structure become near to spheroidal and this could increase the area of the inhibition (Syamsuir et al., 2023a).

According to the above-mentioned data, the research combined between a rise in the current and rotating magnetic fields for Cu electrodeposition is not studied. A few research focused on current densities increment during Cu electrodeposition. Increment of the current densities during electrodeposition would result in different physical properties of the Cu films. Moreover, several researchers conducted electrodeposition Ni by influencing magnetic rotation, which could result in different Cu films physical properties. Combination between current increment and rotation of magnetic field influence would create different Cu films characteristic. Therefore, in the present study, Cu films were made using the electrodeposition technique at various currents (80, 100, and 120 mA), with and without influence by a rotating magnetic field (100 rpm of rotation). In addition, we successfully fabricated the magnetic field influence apparatus during electrodeposition. All Cu films were characterized using X-ray diffraction (XRD), attenuated total reflectance Fourier transform infrared spectroscopy (ATR-FTIR), Scanning electron microscopy equipped with Energy dispersive spectroscopy (SEM-EDS), and Potentiostat apparatus. Furthermore, antibacterial activity using *Staphylococcus aureus* was also investigated.

2. EXPERIMENTAL

2.1 Materials and Instrumentation

The cathode in the present study used Al alloy (20×20×2 mm) with composition 0.106 wt% Si, 0.365 wt% Fe, 0.055 wt% Cu, 0.043 wt% Mn, 0.030 wt% Mg, 0.003 wt% Zn, 0.002 wt% Ni, 0.018 wt% Ti, 0.003 wt% Pb, and Al balance. The anode used for electrodeposition is similar to the previous study (Syamsuir et al., 2024). 0.5 M $CuSO_4$ + 20 mL of H_2SO_4 was used for electrolyte solutions. The electrodeposition was conducted

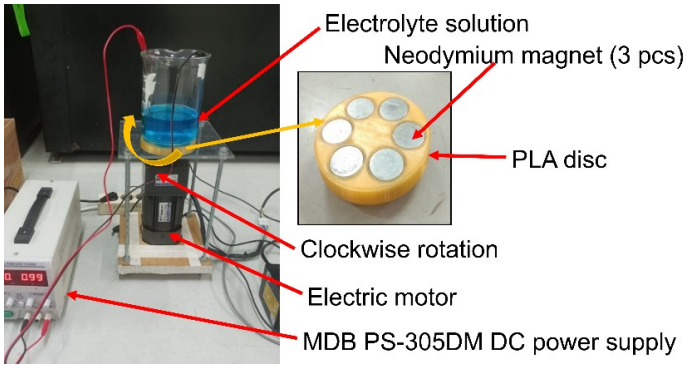

Figure 1. Apparatus for the Electrodeposition Process

using an MDB PS-305DM DC power supply. While magnets were used to influence the electrodeposition process using three neodymium magnets, south pole near to electrolyte solution. One neodymium magnet has 0.08 T of intensity. The completed customized apparatus for fabricated Cu films is presented in Figure 1. Moreover, XRD, ATR-FTIR, SEM-EDS, and potentiostat were conducting using Panalytical AERIS, PerkinElmer, AxiaTM ChemiSEMTM from Thermo Fisher and Digi-Ivy DY 2311, respectively.

2.2 Procedure

Electrodeposition was conducted at room temperature, while the distance between the anode and cathode was fixed set for 5 cm. The electrodeposition was conducted using a DC power supply at 80, 100 and 120 mA for one hour (with and without rotating magnetic influence). For magnetic influence, 100 rpm of speed rotation was conducted. The sample's name was designated without the influence of magnetic fields such as Cu8-0, Cu10-0, and Cu12-0, for samples made using 80, 100, and 120 mA of current, respectively. Moreover, the sample's name was designated with influence magnetic fields (100 rpm) as Cu8-100, Cu10-100, and Cu12-100, for samples synthesized using 80, 100, and 120 mA of current, respectively.

2.3 Analysis

The sample before and after electrodeposition was weighed using digital scale to calculate deposition rate and current efficiency (Syamsuir et al., 2024). Moreover, a XRD was used to analyze the samples and collect information about their phase and crystal structure. The Cu Kα radiation source (λ = 0.15406 nm) was employed in an XRD process, and the test settings were set to 2θ = 20-100° and step size 0.02°. Quantitative analysis of the diffraction pattern was performed using the Rietveld method (Larson and Dreele, 2004). Furthermore, the ATR-FTIR was recorded over a spectral range of 4000-600 cm^{-1}. Next, the surface morphology and phase were investigated using SEM-EDS. According to SEM image, Image J software was used to measure grain distribution and surface roughness.

Corrosion behavior was determined by using the potentiodynamic polarization method. The potentiodynamic polarization was conducted using Potentiostat in 0.9% NaCl (room temperature). The potential was scanned between -1.8 – (+0.06 V) using 1 mV/s of scan rate. Cu films as working electrode (WE), Ag/AgCl as reference electrode (RE) and Pt wire as counter electrode (CE). Collected data were investigated using Tafel extrapolation method to be found corrosion current and potential. The corrosion rate could be calculated similarly to the previous study using corrosion current data (Syamsuir et al., 2024). Furthermore, antibacterial activity using *Staphylococcus aureus* was also investigated similar method to the previous study (Syamsuir et al., 2023b).

3. RESULTS AND DISCUSSION

3.1 Deposition Rate and Current Efficiency

Figure 2 presents the Cu deposition rate and current efficiency. The shift to more current led to an increase in deposition rate and cathodic current efficiency. Presenting a rotating magnetic field also enhances both deposition rate and current efficiency. The deposition rates of Cu8-0, Cu8-100, Cu10-0, Cu10-100, Cu12-0, and Cu12-100 samples are 26.51, 27.90, 32.09, 32.92, 37.39, and 37.95 µm/h, respectively. Meanwhile, the cathodic current efficiency of Cu8-0, Cu8-100, Cu10-0, Cu10-100, Cu12-0, and Cu12-100 samples are 30.82, 32.44, 53.89, 55.29, 86.94, and 88.24%, respectively.

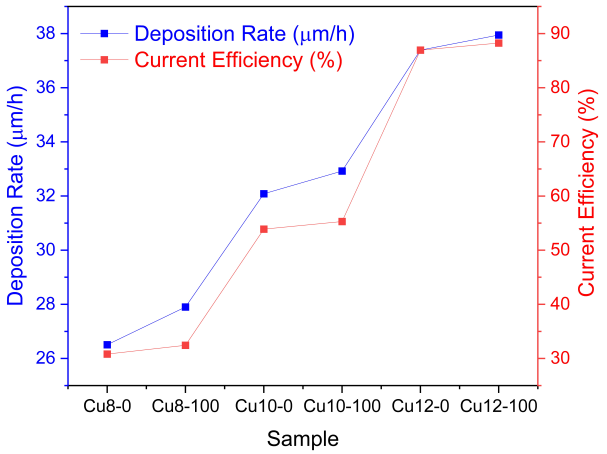

Figure 2. Deposition Rate and Current Efficiency of Cu Electrodeposition

An increase in deposition current leads to more throwing power, so Cu ion placed more on the cathode surface. Therefore, the deposition rate increases linearly to the current (SEAKR, 2017). Ye et al. (2023) have found increasing the deposition potential leads to an increase in the deposition rate. Augustin et al. (2016a) have found that deposition of Cu using 2 A/dm^2 for 10 min resulting the Cu not covering all Al surface, while at 10 A/dm^2 all Al surface was fully covered with Cu. This indicates a lower current resulting lower deposition rate, therefore, for 10 min time deposition could not cover all Al alloy surfaces. Another study has found that increased current for various Cu electrolyte solutions leads to an increase in deposition rate (SEKAR, 2017).

Higher current led to an increase in the current efficiency. Some researchers have found current efficiency would decrease at higher current density (4 A/dm^2) (SEAKR, 2017). This condition was significantly influenced by hydrogen evolution happening on the surface of the cathode. The hydrogen evolution could act as a barrier for Cu ions coming to the cathode surface, therefore current efficiency is decreased.

Moreover, the deposition rate and current efficiency are increased by presenting a magnetic field rotation. This indicates the Eddy electric field induces the Cu ion to move faster to the cathode. According to Wang et al. Eddy electric field could act as MHD flow convection, therefore it increases the deposition rate and current efficiency (Wang and Chen, 2015). Another force that influences the current efficiency and deposition rate is the paramagnetic force (Park et al., 2008). Furthermore, Chiba et al have found, that presenting a magnetic field (0.12 T) could enhance the current efficiency by more than 100% (Chiba et al., 1988).

3.2 XRD Analysis

Figure 3 shows the pattern data obtained from the XRD recording of six samples of Cu electrodeposition on Al substrates. The face-centered cubic (fcc) Cu phase can be identified by

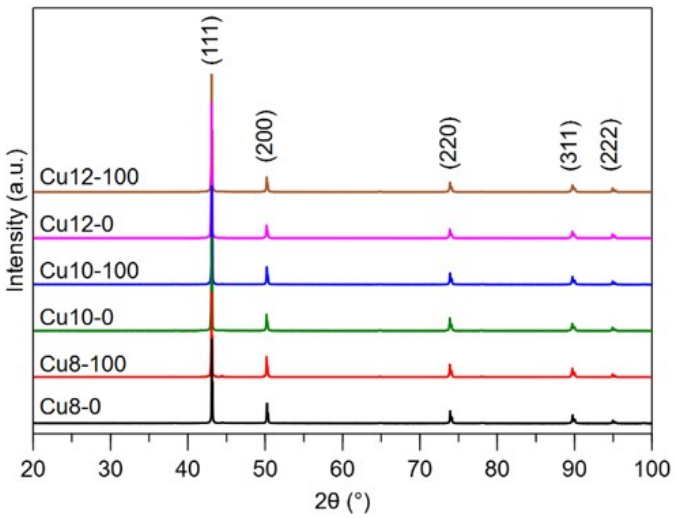

Figure 3. Diffraction Patterns of the Cu Films

the reflection of the diffraction peaks of (111) (43.09°), (200) (50.22°), (220) (73.92°), (311) (89.75°), and (222) (94.96°) based on the research findings. These samples have the same peaks of the Cu phase oriented in the (111) plane as those reported by other researchers (Li et al., 2022; Sen et al., 2003; Yonezawa et al., 2015). Based on the results, it appears that Cu has been successfully deposited onto the Al surface. According to the calculations of the lattice parameters for the Cu phase (space group F m -3 m), all six samples have a lattice parameter of 0.3616 nm. Despite changes in current or magnetic fields, the fcc Cu crystal seems to maintain its orientation and structure.

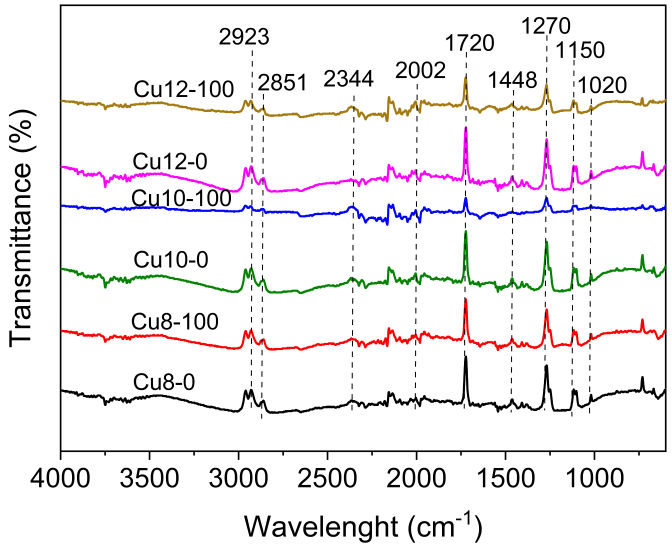

Figure 4. ATR-FTIR Spectral of the Cu Films

3.3 ATR-FTIR Analysis

Figure 4 shows the IR spectrum of the various samples. The peaks at 2923 and 2851 cm^{-1} correspond to C−H stretching vibration of the CH_2 groups (Kayani et al., 2022). Band registered at 2344 cm^{-1} is assigned to CO_2 in atmosphere (Kayani et al., 2022). The peak at 2002 cm^{-1} is attributed to the CO_2 and H_2O on the surface of the Cu film (Fuku et al., 2020). The C=O stretching of the carboxyl group appearing at 1720 cm^{-1} (Aguilar-Perez et al., 2020). The peaks at 1448 and 1270 cm^{-1} may be assigned to CO_2Cu and $Cu(CS)_3$, respectively (Hsu et al., 2024; Kong et al., 2003). The band at 1150 cm^{-1} is attributed to C−O bond stretching (Kayani et al., 2022). The C−O stretching frequency of carboxylate ion bond to Cu films is seen at 1020 cm^{-1} (Fuku et al., 2020). Generally, it could be concluded, Cu was successfully deposited onto Al surface due to presenting CO_2Cu and $Cu(CS)_3$ at 1448 cm^{-1} and 1270 cm^{-1}, respectively.

3.4 SEM-EDS Analysis

Figure 5 presents the SEM image of the various samples. A clean surface is seen in the Cu8-0 sample, while other samples exhibit a little black area. Increasing the current led to a change in the surface morphology of the sample which was significantly influenced by deposition rate and current efficiency (Haerifar and Zandrahimi, 2013). Higher deposition rate and current efficiency indicating Cu ions moving faster to the cathode; therefore, the surface morphology is changing. According to Figure 5 currents used for the electrodeposition process between 80-100 mA would result in a faceted structure while using 120 mA results near to spheroidal. Grujicic and Pesic (2002) have found the change in surface morphology due to deposition potential. Deposition potential for 60, 250 and 800 mV would result faceted, spheroidal and dendritic structures, respectively (Fukunaka et al., 1990). Moreover, Ibañez and Fatás (2005) study found current densities of 0.6, 24, and 50 A/dm^2, resulting in surface morphology pyramidal-like, near to spheroidal and spheroidal, respectively.

Generally, presenting a rotating magnetic field leads to surface morphology being more compact. According to Park et al. (2008) presenting a magnetic field would present a paramagnetic field, attracting more Cu ions and thus it could change in surface morphology. Moreover, presenting a magnetic field could suppressed the grain, consequently resulting in more compact morphology (Morimoto et al., 2004). Previous studies have found that presenting magnetic field rotation during the electrodeposition of Cu leads to more compact surface morphology (Syamsuir et al., 2023a).

Figure 6 presents the EDS curve of various samples and Table 1 shows the quantitative result of the EDS curve. The EDS investigation is based on the SEM area in Figure 5. Generally, presenting magnetic field rotation led to an increase in carbon (C) content. While the oxygen (O) content is dependent on the presenting magnetic field rotation.

For a deeper investigation of a little black area in Figure 5, an EDS investigation was conducted. Figure 7 presents the

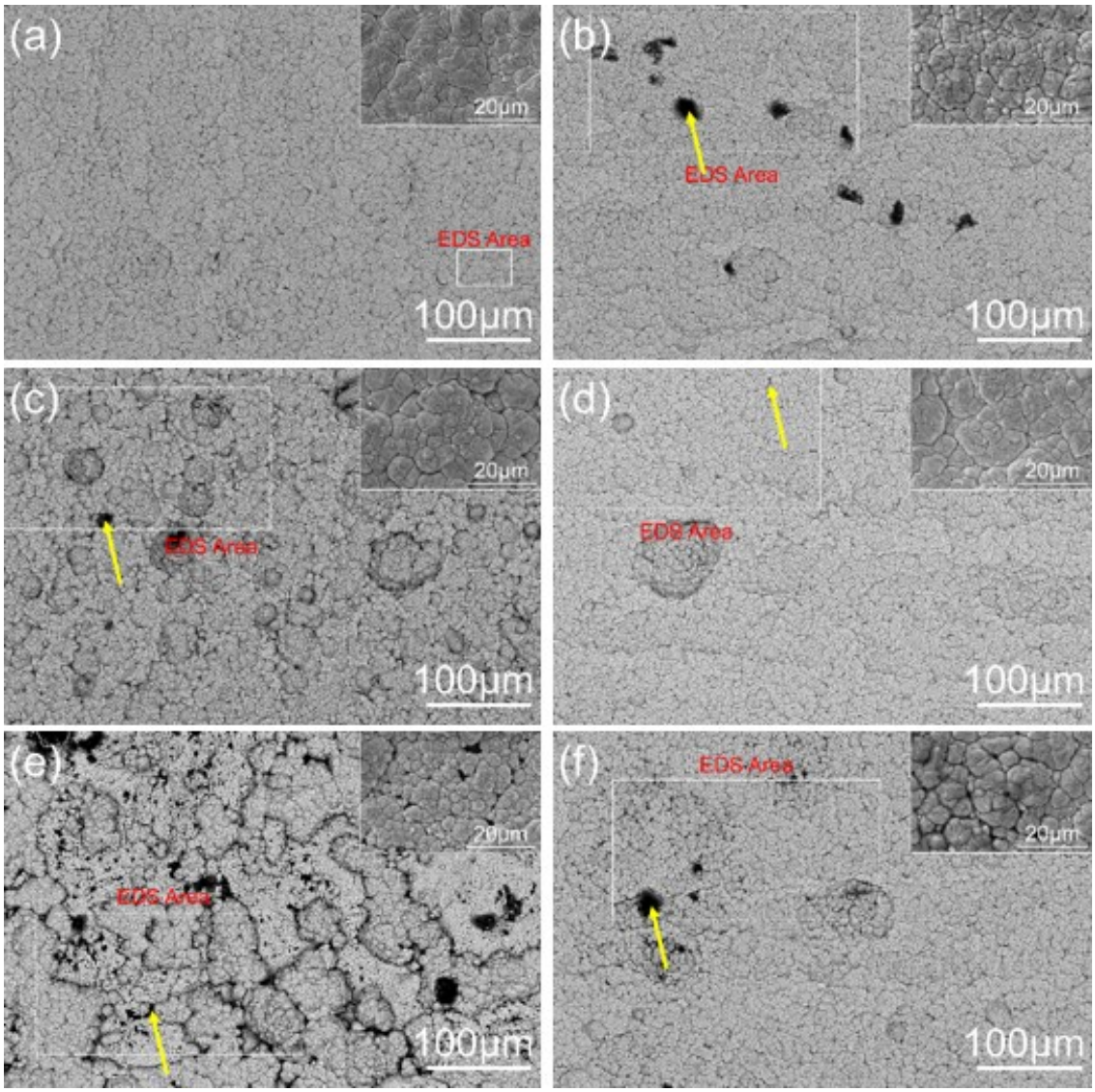

Figure 5. SEM Result of Cu Films (a) Cu8-0, (b) Cu8-100, (c) Cu10-0, (d) Cu10-100, (e) Cu12-0, and (f) Cu12-100

Table 1. Founded Phase According to EDS Investigation of Cu Films

Sample	Phase (wt.%)		
	C	O	Cu
Cu8-0	8.1	0.4	91.5
Cu8-100	10.8	3.1	86.1
Cu10-0	7.7	0.5	91.8
Cu10-100	8.1	0.7	91.2
Cu12-0	7.9	2.0	90.1
Cu12-100	15.8	0.9	83.3

EDS curve of the little black area on various samples and Table 2 shows the quantitative result of the EDS curve. Several C phases are seen in the little black area. The Cu12-0 sample showing the Al phase that indicates Al alloy is not fully covered by Cu film (exhibits a porosity).

Figure 8 presents the grain distribution of various Cu films samples. Shifting to higher currents leads to decrease in grain sizes. Meanwhile, presenting a rotating magnetic field also enhances the grain size. A wider grain size is found in the Cu8-100 sample, while a narrow grain size is seen in the Cu12-0 sample. An increase in the current deposition leads to an increase in deposition rate; the forming grain narrower (Niu et al., 2015). Wang et al. (2015) study also found similar behavior, an increase in the current during Cu electrodeposition leads to a decrease in the grain size. Although presenting a rotating magnetic field increases the deposition rate, the grain is becoming wider. This behavior was influenced by the magnetic field that induced the Cu ions. Increasing the deposition rate by presenting a rotating magnetic field is influenced by paramag-

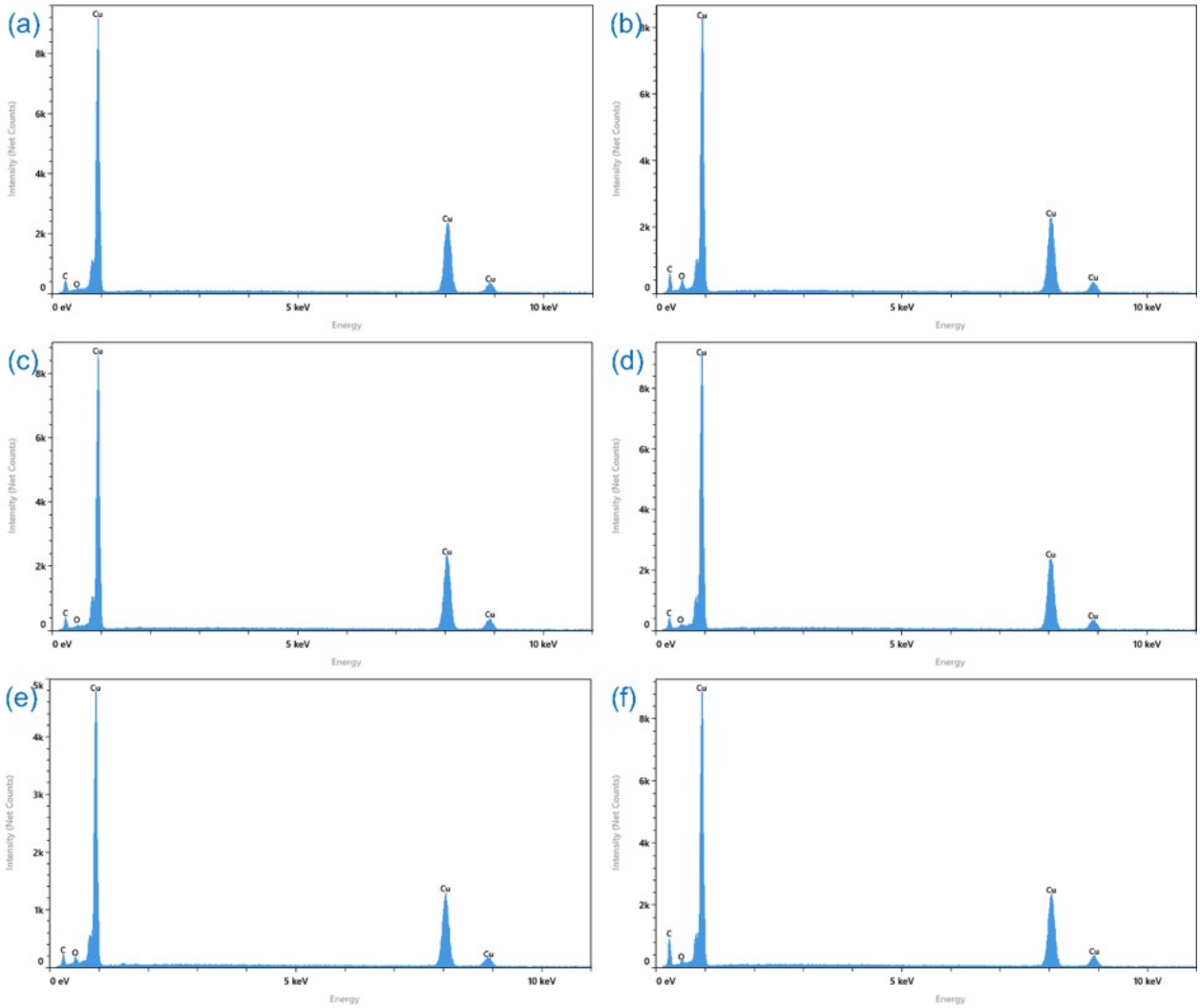

Figure 6. EDS Curve of Cu films (a) Cu8-0, (b) Cu8-100, (c) Cu10-0, (d) Cu10-100, (e) Cu12-0, and (f) Cu12-100

Table 2. Phase Found According to Additional EDS Investigation Black Spot-on Cu Films

Sample	Phase (wt. %)										
	C	N	O	Mg	Al	Si	S	Cl	Ca	Fe	Cu
Cu8-100	35.8	9.6	21.2	-	-	0.4	0.7	2.5	-	-	29.8
Cu10-0	26.8	-	21.8	-	-	-	-	-	-	-	51.4
Cu10-100	13.3	2.3	25.9	0.3	4.0	5.2	-	0.4	0.9	0.7	47.0
Cu12-0	5.5	-	3.7	-	89.1	-	-	-	-	-	1.7
Cu12-100	70.0	8.7	17.5	-	-	0.1	0.2	-	-	-	3.3

netic force (Park et al., 2008). While wider grain is influenced by Lorentz force where resulting magnetohydrodynamic effect (Mogi et al., 2013). The magnetohydrodynamic effect is arranged Cu ions when it arrives at the cathode, therefore wider grain is formed (Morimoto et al., 2004).

Figure 9 presents the surface roughness of various Cu films. Shifts to more current led to an increase in surface roughness. Armini (2011) has found that an increase in the current density (from 3 to 4 mA/cm^2) of the Cu electrodeposition using 0.04 M $CuSO_4$ leads to an increase in the surface roughness. Presenting a rotating magnetic field also enhances surface roughness. The surface roughness of Cu8-0, Cu8-100, Cu10-0, Cu10-100, Cu12-0, and Cu12-100 samples are 20.02, 22.04, 20.58, 23.67, 30.82, and 38.97 µm, respectively. High surface roughness due to gradient concentration increases between cathode and electrolyte solution. Several forces induce

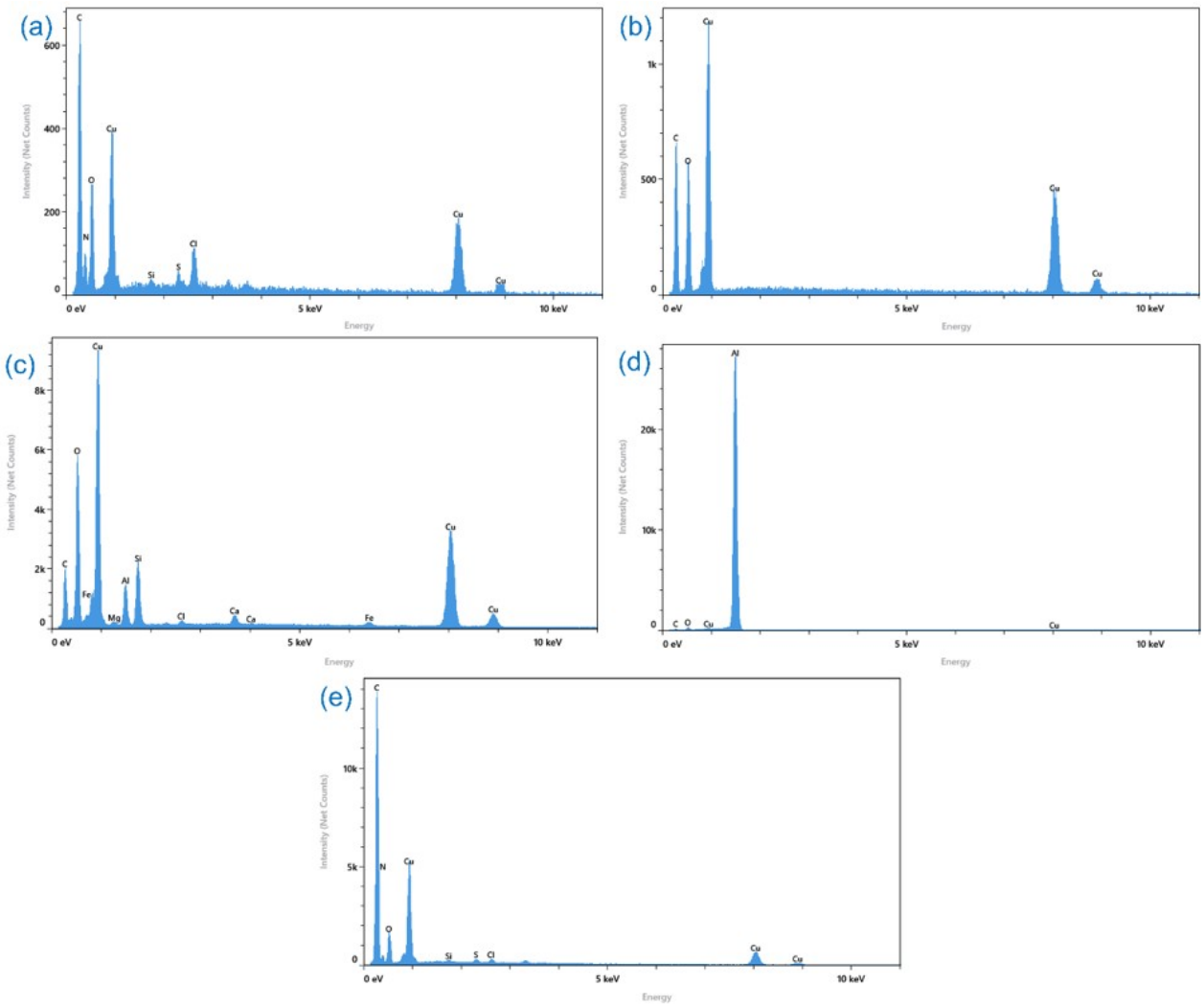

Figure 7. Additional EDS Investigation Black Spot-on Cu Films (a) Cu8-100, (b) Cu10-0, (c) Cu10-100, (d) Cu12-0, and (e) Cu12-100

these gradient concentrations such as paramagnetic and Lorent forces (Park et al., 2008). Presenting rotating magnetic fields tends to present this force, implying more roughness would form. Generally, roughness between 19.6 - 22.04 μm due to the surface morphology was formed in the faceted structure. While 30.82 and 38.97 μm of surface roughness value due to the surface morphology were formed is spheroidal. Therefore, the spheroidal form can be concluded resulting in surface morphology more roughness than faceted structure.

3.5 Potentiodynamic Polarization

Figure 10 represents the potentiodynamic polarization test resulting in 0.9% NaCl. Corrosion parameters are summarized in Table 3. According to Table 3, corrosion potential (Ecorr) is independent of the corrosion rate. Cu8-100 has a more positive value than other samples (nobler), while Cu8-0 has a more negative value of Ecorr than other samples. This indicates that Cu8-0 has more cathodic, and Cu8-100 has more anodic than other samples. In several cases, more anodic samples would result in a higher corrosion rate, while more cathodic samples would result in a lower corrosion rate (Syamsuir et al., 2023a).

Table 3. Corrosion Parameters of Cu Films

Sample	Ecorr (V) vs Ag/AgCl	Icorr (A/cm^2)	Corrosion rate (mmpy)
Cu8-0	-0.566	1.64×10^{-4}	0.949
Cu8-100	-0.298	9.21×10^{-4}	5.430
Cu10-0	-0.463	3.87×10^{-4}	2.240
Cu10-100	-0.506	4.22×10^{-4}	2.450
Cu12-0	-0.484	2.13×10^{-4}	1.240
Cu12-100	-0.474	1.39×10^{-4}	0.808

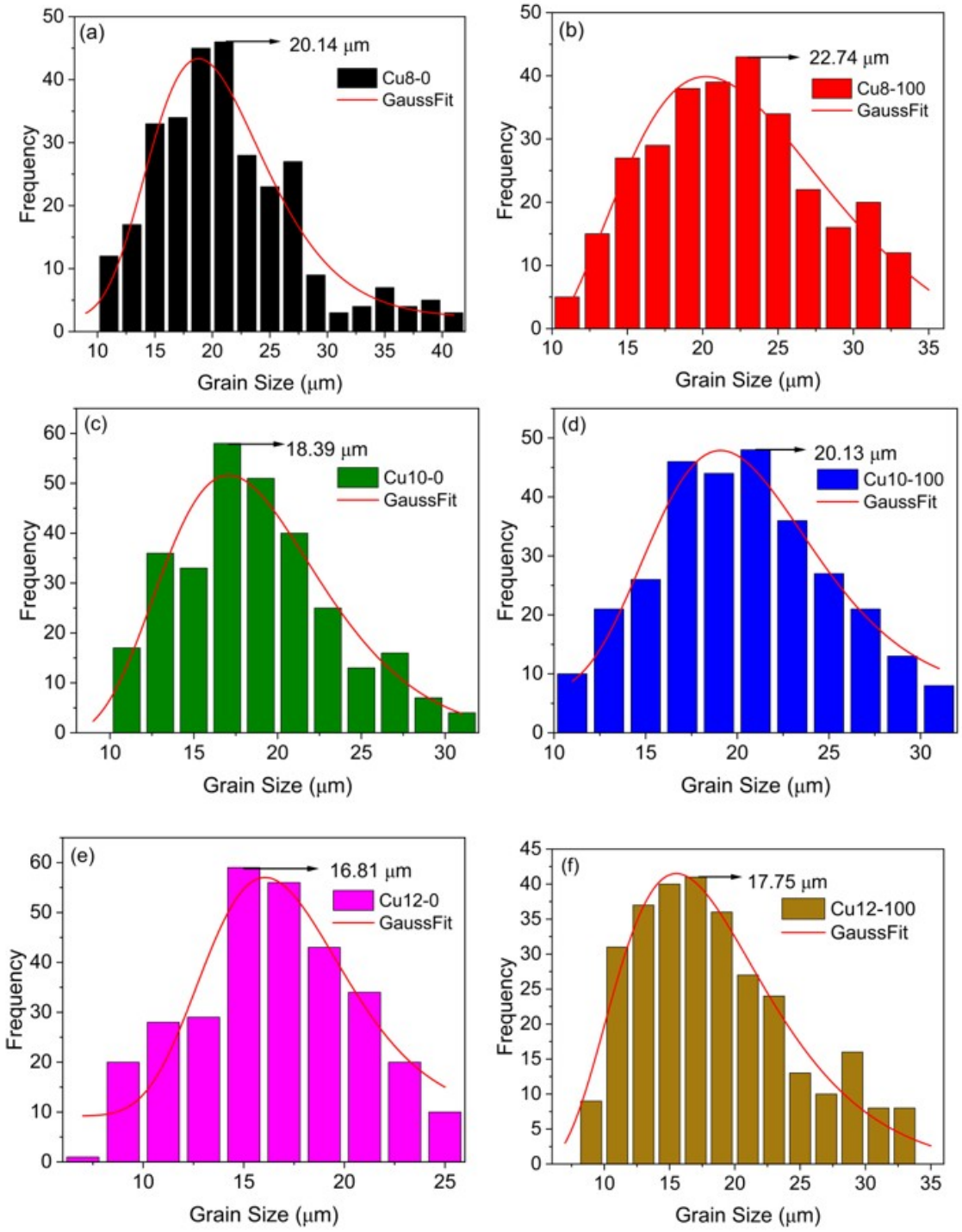

Figure 8. Grain Distribution of Cu Films (a) Cu8-0, (b) Cu8-100, (c) Cu10-0, (d) Cu10-100, (e) Cu12-0, and (f) Cu12-100

Corrosion in NaCl medium is a dissolution of the Cu resulting in CuCl on the Cu surface in the first stage. The CuCl has poor adhesion and, therefore, it could not protect the Cu surface from aggressive chloride ions. This condition makes the CuCl transform into Cu(I)Cl complex and then dissolve in the chloride solution (Li et al., 2011; Sudheer and Quraishi, 2013; Wang et al., 2014). According to Table 3, the best corrosion resistance is seen in the Cu12-100 sample, which indicates the Cu film has a slower chemical reaction (dissolve) than others (Tasic et al., 2018).

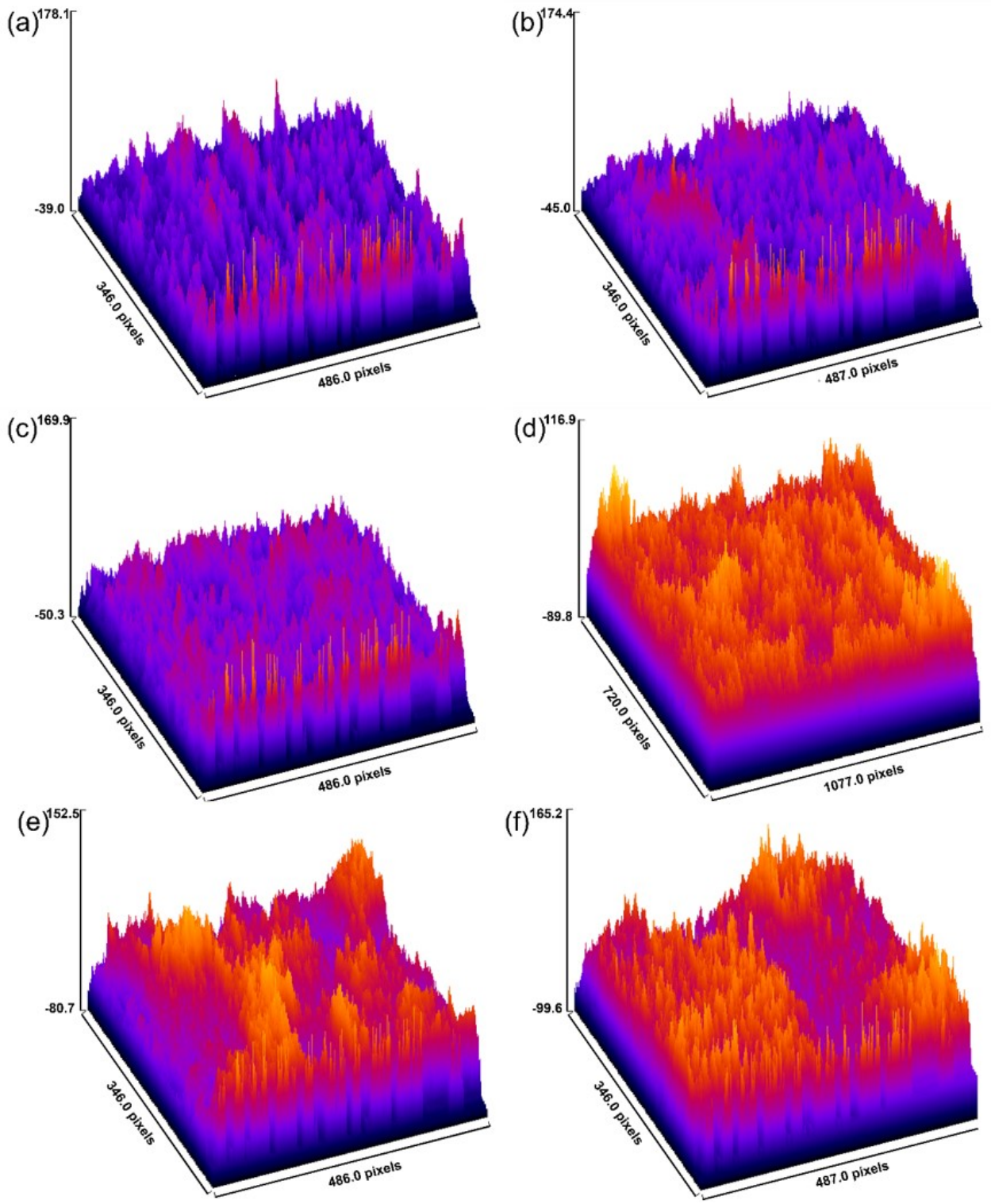

Figure 9. Surface Roughness of Cu Films (a) Cu8-0, (b) Cu8-100, (c) Cu10-0, (d) Cu10-100, (e) Cu12-0, and (f) Cu12-100

3.6 Antibacterial Activity

Figure 11 represents antibacterial activity investigation on Cu Films using *Staphylococcus aureus*. Diffusible metal observation results of Cu films are summarized in Table 4. Presenting magnetic field rotation during electrodeposition led to a decreased area of inhibition for samples, which was made using 80 mA of current. Samples made using 100 and 120 mA of current, presenting magnetic field rotation that led to an increased area

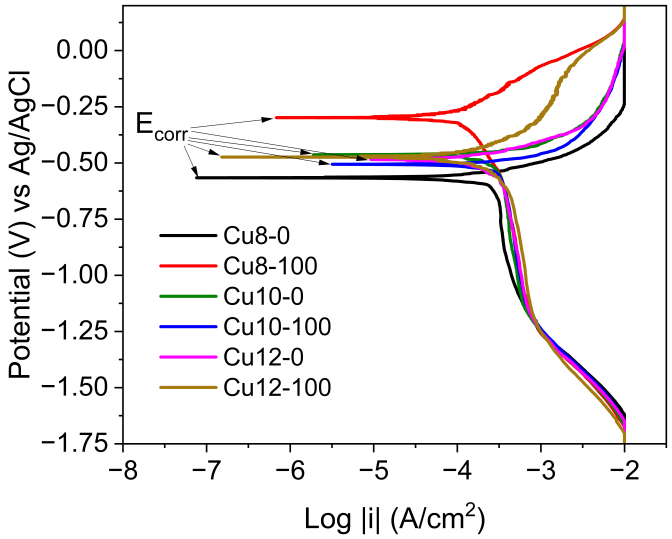

Figure 10. Potentiodynamic Polarization Curve of Cu Films

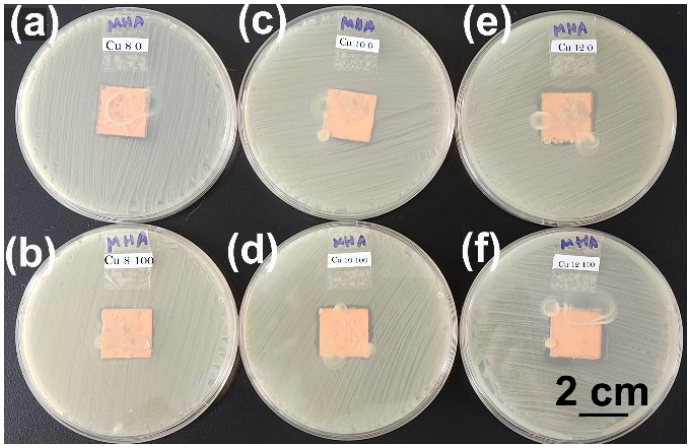

Figure 11. Antibacterial Activity Investigation on Cu Films (a) Cu8-0, (b) Cu8-100, (c) Cu10-0, (d) Cu10-100, (e) Cu12-0, and (f) Cu12-100

of inhibition. The higher area of inhibition is seen in the Cu12-100 sample, while the lower area of inhibition is seen in the Cu8-100 sample.

Table 4. Diffusible Metal Observation on Cu Films

Sample	Kill area (cm^2)	Area of inhibition (cm^2)
Cu8-0	5.90 ± 0.17	1.63
Cu8-100	5.60 ± 0.83	0.89
Cu10-0	5.79 ± 0.75	1.61
Cu10-100	6.34 ± 0.37	1.91
Cu12-0	6.79 ± 0.20	2.26
Cu12-100	8.63 ± 0.51	4.01

The area of inhibition was significantly influenced by Cu ions released from the samples. Higher releasing ions could enhance the area of inhibition (Fatimah et al., 2025). According to Raja et al. (2023), more Cu concentration leads to an increased area of inhibition. Comparing Table 4 to Figure 2, Cu films made using 120 mA of current have a higher deposition rate and current efficiency, thus they have more thickness and higher area of inhibition. Shim et al. (2015) have found that a thick layer resulting higher bacteria killing efficiency. Moreover, comparing Table 4 to the SEM image, the group sample synthesis using 120 mA has a higher area of inhibition than others. Probably it is due to the near spheroidal surface morphology being formed. Although the faceted structure has a wider grain size than near to spheroidal (confirmed by grain distribution analysis), they have a larger surface area proved by more roughness, hence it released more Cu ions on the environment. Along with Tavakoli et al. (2019), a bigger surface area resulting in more effective to bacterial retardant. Furthermore, more roughness resulting higher killing efficiency, due to more contact between Cu and the bacteria (Shim et al., 2015). According to Figure 9, Cu 12-100 has more roughness than other samples and consequently has a higher inhibition area.

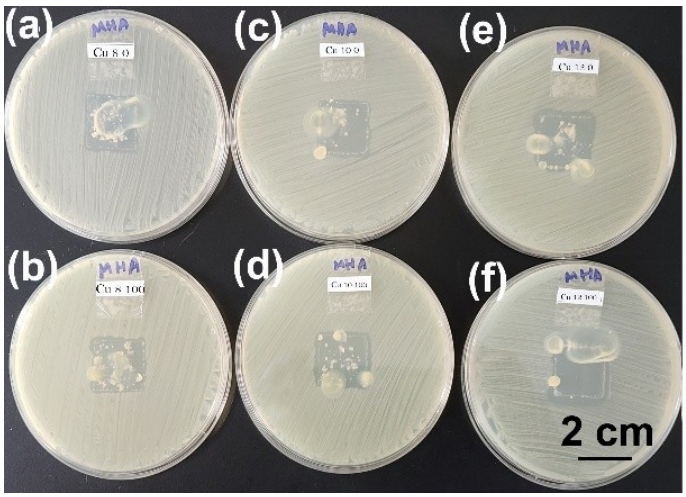

Figure 12. 48-Hour Post Contact Observation of Antimicrobial Activity (a) Cu8-0, (b) Cu8-100, (c) Cu10-0, (d) Cu10-100, (e) Cu12-0, and (f) Cu12-100

After 24 hours, the materials were removed using sterile forceps. Afterwards, the agar is re-incubated at 35C° ±2 for another 24-48 hours. Figure 12 represents a 48-hour post-contact observation of antimicrobial activity using Staphylococcus aureus. After 48 hours of post-contact, the area where the sample was placed still looks sterile from bacterial activity (remain clear). The killing mechanisms of the bacteria using Cu have several ways. (1) Interaction between Cu films and bacteria could damage the bacteria cell wall due to generation of the reactive oxygen species (ROS) such as hydroxyl radicals, hydrogen peroxide, superoxide anions or organic hydroperoxides leading to cell lysis. (2) Released Cu ions from Cu film would attach to the peptidoglycans, carboxylic groups or lipopolysac-

Table 5. Antibacterial Activity Comparison on Cu Using *Staphylococcus aureus*

Method	Inhibition Zone/Kill Area	Reference
CuO nanoparticle modified polyol method (50 µl of CuO)	21 ± 1.612 mm	(Ramyadevi et al., 2012)
Cu foil immersed in 10 mL alkaline solution for 21 days (15×15 mL)	ϕ 25.17 mm	(Ekthammathat et al., 2013)
CuO nanoparticle aqueous precipitation method (750 µg of CuO)	Around 18 mm	(Ahamed et al., 2014)
SKU AA010278 immersed in copper (II) chloride solution for 1–3 min	19 ± 2 mm	(Abdurazova et al., 2017)
Precipitation technique of CuO (200 µg)	7.26 ± 2 mm	(?)
Sol-gel method (CuO 3% in 2.5 Mg/mL)	17.5 ± 0.7 mm	(Kayani et al., 2022)
Cu electrodeposition (ϕ 23 mm)	40 ± 1 mm	(Syamsuir et al., 2023b)
Cu electrodeposition (20 × 20 cm)	8.63 ± 0.51 cm^2	Present study

charides bacteria cell walls, disrupting cell membrane stability and the damaging the intracellular contents (Fatoni et al., 2023; Gilbertson et al., 2016; Kamila et al., 2023; Motshekga, 2024; Salah et al., 2024). Subsequently, in the present study probably the mechanism following second ways, where Cu ions remain in the former sample area, so that it can inhibit bacterial growth.

Table 5 shows comparison of inhibition zone or kill area of various study to the present study. It should be noted that the difficulties compared between them are due to sample dimension (weight). More CuO nanoparticles weight lead to increase the inhibition zone (Ahamed et al., 2014; Selvaraj, 2020). Generally, electrodeposition Cu films using various current and influenced by rotating magnet are promising to change inhibition area.

4. CONCLUSIONS

Cu films made using electrodeposition at various currents (with and without influence by a rotating magnetic field) have been successfully synthesized. Increasing the current of electrodeposition leads to an increase in deposition rate, current efficiency, roughness and a decrease in grain size for both conditions. Currents used for the electrodeposition process between 80-100 mA would result in a faceted structure while using 120 mA results near to spheroidal. Current and rotating magnetic influence does not linearly influence corrosion potential, corrosion rate and anti-bacterial activity. The sample made using higher current and influencing with magnetic field result in less corrosion rate and higher inhibition area. A future recommendation of the present work is conducting higher density to examine the phenomena.

5. ACKNOWLEDGMENT

This research was supported by the Ministry of Education, Culture, Research, and Technology through grand funding Penelitian Fundamental-Reguler with contract number 087/LPPM-UNAS/VI/2024 and 815/LL3/AL.04/2024.

REFERENCES

Abdurazova, P. A., U. B. Nazarbek, A. A. Bolysbek, N. K. Sarypbekova, G. S. Kenzhibayeva, G. A. Kambarova, M. S. Sataev, S. T. Koshkarbaeva, A. B. Tleuova, S. Perni, and P. Prokopovich (2017). Preparation of Photochemical Coatings of Metal Films (Copper, Silver and Gold) on Dielectric Surfaces and Studying Their Antimicrobial Properties. *Colloids and Surfaces A: Physicochemical and Engineering Aspects*, **532**; 63–69

Aguilar-Perez, D., R. Vargas-Coronado, J. M. Cervantes-Uc, N. Rodriguez-Fuentes, C. Aparicio, C. Covarrubias, M. Alvarez-Perez, V. Garcia-Perez, M. Martinez-Hernandez, and J. V. Cauich-Rodriguez (2020). Antibacterial Activity of a Glass Ionomer Cement Doped with Copper Nanoparticles. *Dental Materials Journal*, **39**(3); 389–396

Ahamed, M., H. A. Alhadlaq, M. A. M. Khan, P. Karuppiah, and N. A. Al-Dhabi (2014). Synthesis, Characterization, and Antimicrobial Activity of Copper Oxide Nanoparticles. *Journal of Nanomaterials*, **2014**; 637858

Arendsen, L. P., R. Thakar, and A. H. Sultan (2019). The Use of Copper as an Antimicrobial Agent in Health Care, Including Obstetrics and Gynecology. *Clinical Microbiology Reviews*, **32**(4); 1–28

Armini, S. (2011). Cu Electrodeposition on Resistive Substrates in Alkaline Chemistry: Effect of Current Density and Wafer RPM. *Journal of The Electrochemical Society*, **158**(6); D390–D394

Augustin, A., P. Huilgol, K. R. Udupa, and K. U. Bhat (2016a). Effect of Current Density During Electrodeposition on Microstructure and Hardness of Textured Cu Coating in the Application of Antimicrobial Al Touch Surface. *Journal of the Mechanical Behavior of Biomedical Materials*, **63**; 352–360

Augustin, A., K. R. Udupa, and K. U. Bhat (2016b). Effect of Coating Current Density on the Wettability of Electrodeposited Copper Thin Film on Aluminum Substrate. *Perspectives in Science*, **8**; 472–474

Chiba, A., T. Ogawa, and T. Yamashita (1988). Magnetic Field Effects on the Electrodeposition of Copper from Copper Sulphate in Sulphuric Acid. *Surface and Coatings Technology*,

34(4); 455–462
Ekthammathat, N., T. Thongtem, and S. Thongtem (2013). Antimicrobial Activities of CuO Films Deposited on Cu Foils by Solution Chemistry. *Applied Surface Science*, **277**; 211–217
Fatimah, I., N. Nurlaela, A. Z. Fauziyyah, S. Sagadevan, H. Hidayat, M. N. M. Haneef, M. F. Daud, A. Kamari, and W. C. Oh (2025). Clitoria Ternatea Flower Extract Mediated Synthesis of Ni-Doped Hydroxyapatite as Photocatalyst, Antibacterial, and Drug Delivery Agent for Anticancer Drug. *Science and Technology Indonesia*, **10**(2); 360–373
Fatoni, A., A. Rendowati, L. Sirumapea, L. Miranti, S. Masitoh, and N. Hidayati (2023). Synthesis, Characterization of Chitosan-ZnO/CuO Nanoparticles Film, and Its Effect as an Antibacterial Agent of *Escherichia coli*. *Science and Technology Indonesia*, **8**(3); 373–381
Fuku, X., M. Modibedi, and M. Mathe (2020). Green Synthesis of Cu/Cu_2O/CuO Nanostructures and the Analysis of Their Electrochemical Properties. *SN Applied Sciences*, **2**(5); 1–15
Fukunaka, Y., H. Doi, and Y. Kondo (1990). Structural Variation of Electrodeposited Copper Film with the Addition of an Excess Amount of H_2SO_4. *Journal of The Electrochemical Society*, **137**(1); 88–93
Gilbertson, L. M., E. M. Albalghiti, Z. S. Fishman, F. Perreault, C. Corredor, J. D. Posner, M. Elimelech, L. D. Pfefferle, and J. B. Zimmerman (2016). Shape-Dependent Surface Reactivity and Antimicrobial Activity of Nano-Cupric Oxide. *Environmental Science and Technology*, **50**(7); 3975–3984
Goranova, D., R. Rashkov, G. Avdeev, and V. Tonchev (2016). Electrodeposition of Ni–Cu Alloys at High Current Densities: Details of the Elements Distribution. *Journal of Materials Science*, **51**(18); 8663–8673
Grujicic, D. and B. Pesic (2002). Electrodeposition of Copper: The Nucleation Mechanisms. *Electrochimica Acta*, **47**(18); 2901–2912
Haerifar, M. and M. Zandrahimi (2013). Effect of Current Density and Electrolyte pH on Microstructure of Mn–Cu Electroplated Coatings. *Applied Surface Science*, **284**; 126–132
Hsu, J., M. S. E. Houache, Y. Abu-Lebdeh, R. A. Patton, M. I. Guzman, and H. A. Al-Abadleh (2024). In Situ Electrochemistry of Formate on Cu Thin Films Using ATR-FTIR Spectroscopy and X-ray Photoelectron Spectroscopy. *Langmuir*, **40**(4); 2377–2384
Ibañez, A. and E. Fatás (2005). Mechanical and Structural Properties of Electrodeposited Copper and Their Relation with the Electrodeposition Parameters. *Surface and Coatings Technology*, **191**(1); 7–16
Ji, R., K. Han, H. Jin, X. Li, Y. Liu, S. Liu, T. Dong, B. Cai, and W. Cheng (2020). Preparation of Ni–SiC Nano-Composite Coating by Rotating Magnetic Field-Assisted Electrodeposition. *Journal of Manufacturing Processes*, **57**; 787–797
Kamila, E. A., Z. Abidin, I. I. Arief, and Trivadila (2023). Synthesis, Characterization, Antibacterial Activity, and Potential Water Filter Application of Copper Oxide/Zeolite Composite. *Makara Journal of Science*, **27**(3); 186–193
Kayani, Z. N., M. Ashfaq, S. Riaz, and S. Naseem (2022). Impact of Cu on Structural, Optical, Dielectric Properties and Antibacterial Activity of TiO_2 Thin Films. *Optical Materials*, **132**; 112809
Kong, Q., A. Zeng, M. Chen, M. Zhou, and Q. Xu (2003). Infrared Spectra and Density Functional Calculations of the Copper Thiocarbonyls: CuCS, $Cu(CS)_2$, and Cu_2CS in Solid Argon. *Journal of Chemical Physics*, **118**(16); 7267–7272
Larson, A. C. and R. B. V. Dreele (2004). General Structure Analysis System (GSAS). Technical Report Vol. 748, Los Alamos
Li, W., L. Hu, S. Zhang, and B. Hou (2011). Effects of Two Fungicides on the Corrosion Resistance of Copper in 3.5% NaCl Solution Under Various Conditions. *Corrosion Science*, **53**(2); 735–745
Li, Z., B. Tan, J. Luo, J. Qin, G. Yang, C. Cui, and L. Pan (2022). Structural Influence of Nitrogen-Containing Groups on Triphenylmethane-Based Levelers in Super-Conformal Copper Electroplating. *Electrochimica Acta*, **401**; 139445
Liu, Y., B. Zheng, T. Zhang, Y. Chen, J. Liu, Z. Wang, and X. Gong (2022). Magnetic Field Intensified Electrodeposition of Low-Concentration Copper Ions in Aqueous Solution. *Electrochimica Acta*, **432**; 141201
Mogi, I., R. Morimoto, R. Aogaki, and K. Watanabe (2013). Surface Chirality Induced by Rotational Electrodeposition in Magnetic Fields. *Scientific Reports*, **3**; 2574
Morimoto, R., A. Sugiyama, and R. Aogaki (2004). Nano-Scale Crystal Formation in Copper Magneto-Electrodeposition Under Parallel Magnetic Fields. *Electrochemistry*, **72**(6); 421–423
Motshekga, S. C. (2024). Structural and Antibacterial Properties of Copper Oxide Nanoparticles: A Study on the Effect of Calcination Temperature. *Nano Express*, **5**(1); 015011
Murdoch, H. A., D. Yin, E. Hernández-Rivera, and A. K. Giri (2018). Effect of Applied Magnetic Field on Microstructure of Electrodeposited Copper. *Electrochemistry Communications*, **97**; 11–15
Niu, J., X. Liu, K. Xia, L. Xu, Y. Xu, X. Fang, and W. Lu (2015). Effect of Electrodeposition Parameters on the Morphology of Three-Dimensional Porous Copper Foams. *International Journal of Electrochemical Science*, **10**(9); 7331–7340
Park, B. N., Y. S. Sohn, and S. Y. Choi (2008). Effects of a Magnetic Field on the Copper Metallization Using the Electroplating Process. *Microelectronic Engineering*, **85**(2); 308–314
Raja, F. N. S., T. Worthington, and R. A. Martin (2023). The Antimicrobial Efficacy of Copper, Cobalt, Zinc and Silver Nanoparticles: Alone and in Combination. *Biomedical Materials (Bristol)*, **18**; 045003
Ramyadevi, J., K. Jeyasubramanian, A. Marikani, G. Rajakumar, and A. A. Rahuman (2012). Synthesis and Antimicrobial Activity of Copper Nanoparticles. *Materials Letters*, **71**; 114–116

Salah, I., E. Allan, S. P. Nair, and I. P. Parkin (2024). Antibacterial Performance of a Copper Nanoparticle Thin Film. *Nano Select*, **5**(9); 1–13

SEAKR, R. (2017). Microstructure and Crystallographic Characteristics of Nanocrystalline Copper Prepared from Acetate Solutions by Electrodeposition Technique. *Transactions of Nonferrous Metals Society of China (English Edition)*, **27**(6); 1423–1430

SEKAR, R. (2017). Synergistic Effect of Additives on Electrodeposition of Copper from Cyanide-Free Electrolytes and Its Structural and Morphological Characteristics. *Transactions of Nonferrous Metals Society of China (English Edition)*, **27**(7); 1665–1676

Selvaraj, S. P. (2020). Enhanced Surface Morphology of Copper Oxide (CuO) Nanoparticles and Its Antibacterial Activities. *Materials Today: Proceedings*, **50**; 2865–2868

Sen, P., J. Ghosh, A. Abdullah, P. Kumar, and Vandana (2003). Preparation of Cu, Ag, Fe and Al Nanoparticles by the Exploding Wire Technique. *Journal of Chemical Sciences*, **115**; 499–508

Sharifahmadian, O., H. R. Salimijazi, M. H. Fathi, J. Mostaghimi, and L. Pershin (2013). Relationship Between Surface Properties and Antibacterial Behavior of Wire Arc Spray Copper Coatings. *Surface and Coatings Technology*, **233**; 74–79

Shim, G. I., S. H. Kim, H. W. Eom, and S. Y. Choi (2015). Concentration and Roughness-Dependent Antibacterial and Antifungal Activities of CuO Thin Films and Their Cu Ion Cytotoxicity and Elution Behavior. *Journal of Industrial Microbiology and Biotechnology*, **42**(5); 735–744

Sudheer and M. A. Quraishi (2013). Electrochemical and Theoretical Investigation of Triazole Derivatives on Corrosion Inhibition Behavior of Copper in Hydrochloric Acid Medium. *Corrosion Science*, **70**; 161–169

Syamsuir, R. S. Kusumah, A. Premono, A. Lubi, B. Soegijono, S. D. Yudanto, M. K. Ajiriyanto, S. Ismarwanti, R. Kriswarini, C. Rosyidan, D. Nanto, Basori, and F. B. Susetyo (2024). Spinning Effect of Barreling Plating on Physical Properties and Electrochemical Behavior of Copper Layers. *E-Journal of Surface Science and Nanotechnology*, **22**(2); 120–128

Syamsuir, F. B. Susetyo, B. Soegijono, S. D. Yudanto, Basori, M. K. Ajiriyanto, D. Edbert, E. U. M. Situmorang, D. Nanto, and C. Rosyidan (2023a). Rotating-Magnetic-Field-Assisted Electrodeposition of Copper for Ambulance Medical Equipment. *Automotive Experiences*, **6**(2); 290–302

Syamsuir, S., F. B. Susetyo, B. Soegijono, S. D. Yudanto, Basori, and D. Nanto (2023b). Nickel Layers Properties Produced by Electroplating Were Influenced by Spinning Permanent Magnet. *Journal of Physics: Conference Series*, **2596**; 012008

Tasic, Z. Z., M. B. P. Mihajlovic, M. B. Radovanovic, and M. M. Antonijevic (2018). Electrochemical Investigations of Copper Corrosion Inhibition by Azithromycin in 0.9% NaCl. *Journal of Molecular Liquids*, **265**; 687–692

Tavakoli, S., M. Kharaziha, and S. Ahmadi (2019). Green Synthesis and Morphology Dependent Antibacterial Activity of Copper Oxide Nanoparticles. *Journal of Nanostructures*, **9**(1); 163–171

Wang, D., B. Xiang, Y. Liang, S. Song, and C. Liu (2014). Corrosion Control of Copper in 3.5 wt.% NaCl Solution by Domperidone: Experimental and Theoretical Study. *Corrosion Science*, **85**; 77–86

Wang, H., P. Cheng, H. Wang, R. Liu, L. Sun, Q. Rao, Z. Wang, T. Gu, and G. Ding (2015). Effect of Current Density on Microstructure and Mechanical Property of Cu Micro-Cylinders Electrodeposited in Through Silicon Vias. *Materials Characterization*, **109**; 164–172

Wang, T. and W. Chen (2015). Effects of Rotating Magnetic Fields on Nickel Electro-Deposition. *ECS Electrochemistry Letters*, **4**(6); D14–D17

Ye, P., Q. Niu, and F. Wang (2023). Effect of Electrolyte Composition and Deposition Voltage on the Deposition Rate of Copper Microcolumns Jet Electrodeposition. *Materials Science and Engineering: B*, **298**; 116857

Yonezawa, T., Y. Uchida, and H. Tsukamoto (2015). X-Ray Diffraction and High-Resolution TEM Observations of Biopolymer Nanoskin-Covered Metallic Copper Fine Particles: Preparative Conditions and Surface Oxidation States. *Physical Chemistry Chemical Physics*, **17**(48); 32511–32516

